



## International Conference on Electrical Machines and Systems

Oct.17-20, 2008, Shangri-La Hotel, Wuhan, China

[Home](#) ▾

[Welcome Message](#) ▾

[Conference Overview](#) ▾

[Committees](#) ▾

[Technical Program](#) ▾

[Search](#) ▾

[Help](#) ▾

### • Search

Author name ▾

Suk-Hee Lee

SEARCH >>

CLEAR CONDITIONS >>

- |   |   |
|---|---|
| <input type="radio"/> Keynote Speech                                  | <input type="radio"/> Conventional Machines: IM, Sync. and DC Machines, etc |
| <input type="radio"/> Designing, Manufacturing, Testing and Standards | <input type="radio"/> Education for Electric Machinery                      |
| <input type="radio"/> Field Analysis and Computation                  | <input type="radio"/> Heating, Cooling, Vibration, Noise and EMC            |
| <input type="radio"/> High Field Magnet and Applications              | <input type="radio"/> Insulating, Monitoring, Diagnosis and Maintenance     |
| <input type="radio"/> Particle Accelerator and Related Techniques     | <input type="radio"/> Power Electronics, Electric Drives and Motion Control |
| <input type="radio"/> Renewable Energy Generation                     | <input type="radio"/> Special Machines: PM Machines, RM&SRM, LM, etc        |
| <input type="radio"/> Small & Micro Machines, Servos and Actuators    | <input type="radio"/> Theory, Modeling and Simulation                       |
| <input type="radio"/> Transformers, Reactors and Apparatus            |   |

***Tao Sun, Soon-O Kwon, Suk-Hee Lee, Jung-Pyo Hong***

Investigation and Comparison of Inductance Calculation Methods in Interior Permanent Magnet Synchronous Motors



[Top](#)

***Suk-Hee Lee, Geun-Ho Lee, Sung-Il Kim, Jung-Pyo Hong***

A Novel Control Method for Reducing Torque Ripple in PMSM Applied for Electric Power Steering



[Top](#)

# Investigation and Comparison of Inductance Calculation Methods in Interior Permanent Magnet Synchronous Motors

Tao Sun, Soon-O Kwon, Suk-Hee Lee and Jung-Pyo Hong, *Senior Member, IEEE*  
School of Mechanical Engineering, Hanyang University, Seoul, 133-791, Korea

**Abstract**-This paper investigates and compares the inductance evaluation methods for interior permanent magnet synchronous motors (IPMSM). Three major finite element methods will be discussed. First, their detail calculation processes are presented as well as their fundamental principles. Not only the results, but also their solving method, computation time and complexity are compared. Finally, the discussion on the inductance classification is derived, and the calculated results are verified with a series of experiments. The investigation of the calculation methods and the comparison of the evaluated results will be helpful to choose the appropriate inductance calculation method for IPMSM.

## I. INTRODUCTION

Due to the superiorities, such as high power density, wide speed range, and high efficiency, the interior permanent magnet synchronous motors (IPMSM) have been paid much attention. The dominant influences in the correct prediction of the steady-state characteristics and precise vector control for the IPMSM are the d- and q-axis armature inductances and flux linkage of permanent magnet (PM) [1]. The latter can be easily and accurately calculated under no-load condition, which has been demonstrated by many literatures [1], [4]. Because of the nonlinear electromagnetic characteristics including the saturation and cross-coupling effect in the rotor of IPMSM [1]-[4], however, the former becomes much difficult to be evaluated accurately.

In spite of the fact that the corresponding evaluation methods have been discussed for last two decades, there is still no standard for the inductances calculation processes of IPMSM. Although some papers [4], [5] claimed that the accurate results were calculated by analytical methods, the much linearization leads that the available structure is constrained. The finite element analysis (FEA) still is the most trustable method as well known. Among the proposed FEA methods, three kinds can be classified. They are frozen permeabilities method (FPM) [1], vector control method (VCM) [2], and differential flux linkage method (DFM) [3], respectively. According to the results of the previous papers, all these methods can obtain acceptable results. But so far they have been not compared together yet. Based on this purpose, first, this paper will investigate the principle and calculation process of each method so that the solving method of FEA, computation time and complexity can be compared. And

then, depending upon the inductance classification, the analysis results will be discussed.

In addition, the practical test methods also will be briefly discussed. The vector control experiment method will be applied to verify the simulation results and reveal the accuracy of calculation method. The final conclusions of this paper will be helpful to guide motor design and drive researchers to choose proper method to evaluate d- and q-axis inductances of IPMSM as particular situation.

## II. INVESTIGATION OF CALCULATION METHODS

The general definition of inductance is the number of flux linkages in web turns per ampere of current flowing in the coil [6]. In the PM motors, however, the existing flux linkages of PM are superimposed in the flux linkages due to the excited armature currents. Additionally, for the AC motors, most characteristic and dynamic analysis is calculated in the dq-transformation mathematical model. Unfortunately, the dq-model brings more complex calculation in the abstract inductances. In order to solve these problems, the following three methods were proposed.

### A. Frozen Permeabilities Method

As known, the operating point of permanent magnet (PM) varies with the load. It means the flux density and permeability of PM will be different for the different excited current. The PM permeability influences the distribution and saturation of flux linkage which generated by excited armature windings, while the distribution and magnitude of flux linkage also affect the operating point of PM. Therefore, the PM cannot be canceled before the inductance analysis.

Making use of the flexibility of FEA, the authors of [1] proposed a method to calculate the pure flux linkages due to the exciting current by removing the magneto-motive force of PM. The procedure of this method is shown in Fig. 1. First, the nonlinear calculation is processed for each load condition, i.e. certain current and current vector angle. And store the permeability of each element including stator, rotor and PM. Next, by using the stored permeabilities, the stored field energy of motor is calculated by a linear calculation under the corresponding load condition. Finally, the d- and q-axis inductances are calculated by (1).

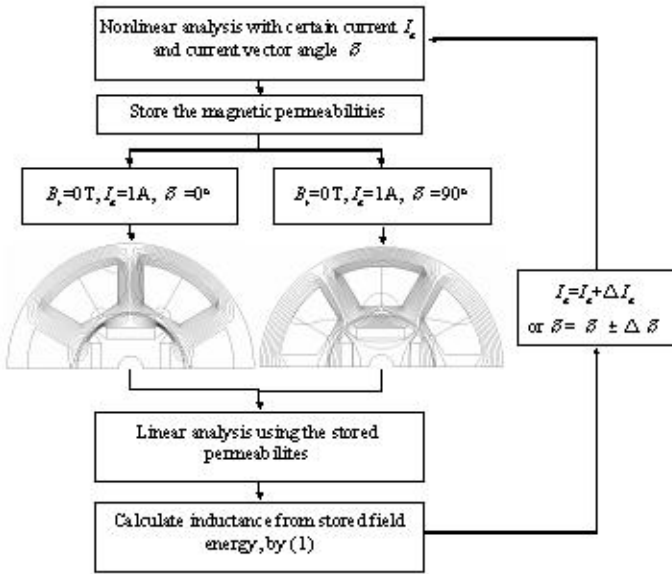


Fig. 1. Procedure of frozen permeabilities method

$$L_{d/q} = \frac{2}{3} \left( \frac{2W_s}{i^2} \right) \quad (1)$$

where  $W_s$  is the stored field energy,  $i$  is the peak value of d- or q-axis currents.

It can be seen that excited current is the source of FEA. Thus, the 2D magneto-static field analysis can be used in this method. Its governing equation is expressed in (2). It is a typical Poisson equation.

$$\nabla \times \left[ \frac{1}{\mu} (\nabla \times \mathbf{A}) \right] = \mathbf{J} \quad (2)$$

where  $\mathbf{A}$  is the magnetic vector potential,  $\mu$  is the isotropic permeability, and  $\mathbf{J}$  is the excited current density of the stator winding. When the model is meshed into about 6500 elements, the computation time this method spent is less than twenty minutes in a computer with Intel Core Due CPU.

### B. Vector Control Method

Depending on the Park's transformation, the IPMSM usually can be expressed in (3).

$$\begin{aligned} v_d &= R_s i_d + L_s \frac{di_d}{dt} - \omega L_q i_q \\ v_q &= R_s i_q + L_q \frac{di_q}{dt} + \omega L_d i_d + \omega \psi_a \end{aligned} \quad (3)$$

And its vector diagram can be described in Fig. 2. In the solid-line part, it can be seen that there are following relationships as described in (4)

$$L_d = \frac{\psi_0 \cos \alpha - \psi_a}{i_d}$$

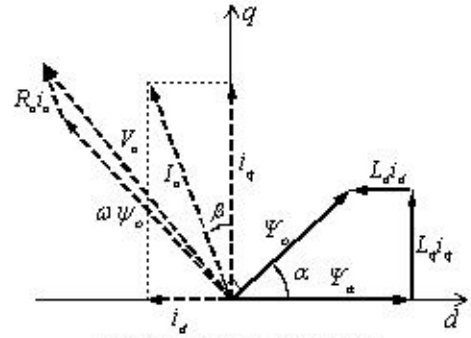


Fig. 2 Vector diagram of IPMSM

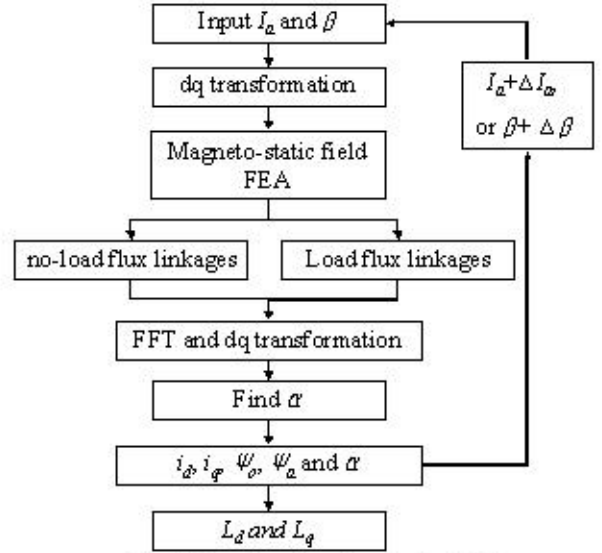


Fig. 3 Procedure of vector control method

$$L_q = \frac{\psi_0 \sin \alpha}{i_q} \quad (4)$$

where  $\psi_a$  is the flux linkage generated by permanent magnet in no-load condition,  $\psi_0$  is the flux linkage generated by permanent magnet and excited armature current, and the  $\alpha$  is the phase shift between the no-load and load back electromotive forces (Back-EMF).

Although the principle is simple, the implement should be paid much attention. First, it is impossible to give d- and q-axis currents directly. The Park's transformation must be processed for every load condition. In addition, these relationships are available without considering the harmonics. Hence, the obtained flux linkages should be filtered by fast Fourier Transform (FFT). The detail calculation procedure of this method can be found in Fig. 3. It is obvious that this method also uses the magneto-static field FEA. But in practice, the computation time needs about several-ten minutes with same computer before, because of the twice nonlinear analysis, FFT, and  $\alpha$  angle searching. It is different to the FPM, the operating point of PM in the VCM is regarded as a constant, and determined at the no-load condition. Therefore, the results of the VCM have inherent error especially at large applied current.

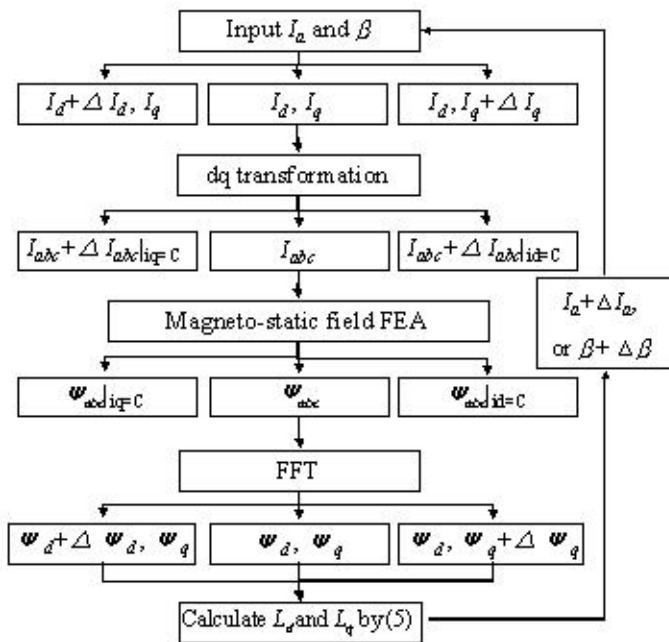


Fig. 4 Procedure of differential flux linkage method

### C. Differential Flux Linkage Method

As mentioned before, the difficulty for calculating the inductance of IPMSM is the existing PM. Furthermore, the operating point of PM also varies with the load condition. The authors of [3] proposed a method to eliminate the PM effect without removing the magneto-motive force like FPM. This method regards the operating points of PM under two near load conditions as the approximately same. Thus, the difference of the flux linkages from two near load condition is totally effect of inductance. Additionally, in order to eliminate the q-axis flux linkage when the d-axis inductance is calculating, the q-axis armature current should be constant, vice versa. Then, the d- and q-axis inductance calculation equations can be calculated by dividing the difference of two near load currents as expressed in (5). The procedure of this method has been shown in Fig. 4.

$$L_d = \left( \frac{\psi_{d1} - \psi_{d2}}{i_{d1} - i_{d2}} \right)_{i_q = \text{const}}$$

$$L_q = \left( \frac{\psi_{q1} - \psi_{q2}}{i_{q1} - i_{q2}} \right)_{i_d = \text{const}} \quad (5)$$

Because the desired variable is the flux linkage, this method can be processed in both magneto-static field FEA and coupled field-circuit FEA, and also can be realized in laboratory experiment [3]. The computation time of this method in magneto-static field FEA is more than that of VCM because more nonlinear calculation steps. The most serious problem of DFM is the determination of the  $\Delta i_{dq}$  in every loop. The much large value will result into very different operating points of PM, while the much small one generates two undistinguishable flux linkages. So far, this method is unstable, and need much artific-

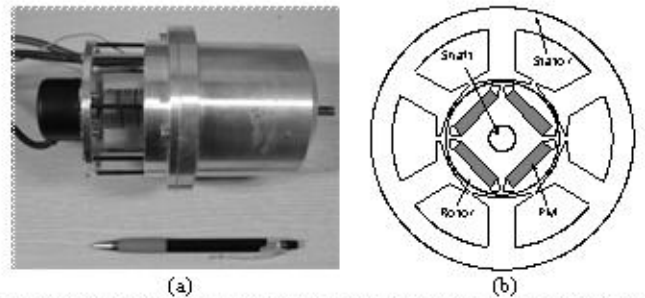


Fig. 5 Analysis motor: (a) photo of analysis motor, (b) cross-section of analysis motor

ial control and verification.

### III. RESULTS COMPARISON AND DISCUSSION

The photo and cross-section of the analysis model are shown in Fig. 5 (a) and (b), respectively. In this paper, the analyzed motor is a spindle-type IPMSM. Its maximum speed is 40000 rpm. The detail dimensions and specification of this motor is shown in Table I.

TABLE I  
Specification of Analysis Motor

Parameter	Value	Unit
Stator outer radii/ Rotor outer radii	79 / 34.5	mm
Airgap length/ Stack length	0.8 / 35	mm
Volume of PM	16×3.5×34	mm <sup>3</sup>
Remanent flux density of PM (@ 20°C)	1.2	T
Recoil permeability	1.05	
Material of core	cogent	
No. of turn in series connected	60	turn
No. of parallel circuits	2	
Rated power	2	kW
Rated current (RMS)	9	A

The d- and q-axis inductances calculated at 6A and 9 A current by the previously mentioned methods are compared and shown in Fig. 6 (a) and (b), respectively. It is obvious that the cross-coupling effect in the d- and q-inductances is not significant. This is because the special tooth structure of the model. In order to reduce the cogging torque, THD of Back-EMF and core losses, the tooth tip is raised referring to the chamber of stator. The much increased effective airgap hence results into a high reluctance in both d- and q-axis so that the flux linkage is not sensitive to the current.

It also can be seen that there are distinguishable differences between the results of each two methods. The inductances calculated by the FPM have the largest value, while those calculated by the DFM are the lowest. Besides the approximation of each method, the different kind of the calculated inductance in each method is the essential reason. As known, the inductance can be classified into three kinds. They are effective inductance, apparent inductance and differential inductance [1], [7]. As shown in Fig. 7, the effective inductance

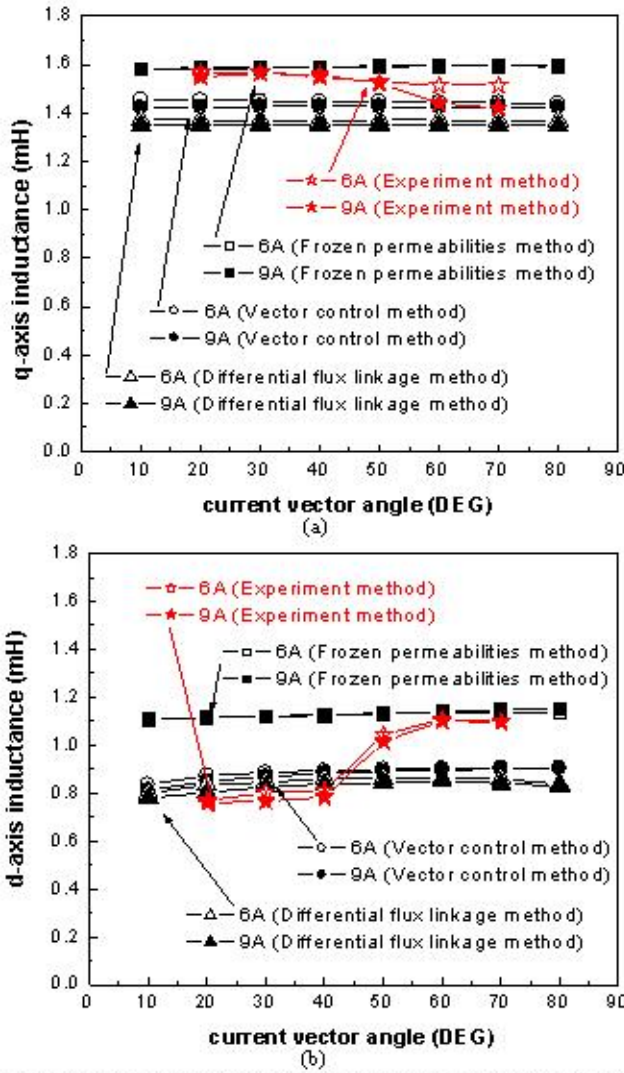


Fig. 6 Calculated inductances: (a) q-axis inductances calculated in the three methods, (b) d-axis inductances calculated in the three methods

is defined as the area of the stored energy at operating point divided by the applied current. It is easy to find that this definition is same to the principle of the FPM. The apparent inductance is defined as its name, the quotient of the present apparent flux linkage divided by the applied current. The VCM essentially is derived from this definition. It also uses the steady-state flux linkage and current. And the differential inductance is the slope of flux linkage at the operating point. It can be expressed in (5), which is the calculation equation of DFM.

It is evident that the linearized apparent flux linkage is larger than the nonlinear stored field energy. Therefore, the apparent inductance should be not lower than the effective inductance. However, it is contrary in the previous calculated results of which the inductances calculated by the FPM are the largest. This is because that the FPM gives only a number of stored field energy in every step, but not a waveform. The number cannot be filtered by FFT, i.e. the contained harmonics cannot be eliminated; while the waveforms calculated by the VCM have

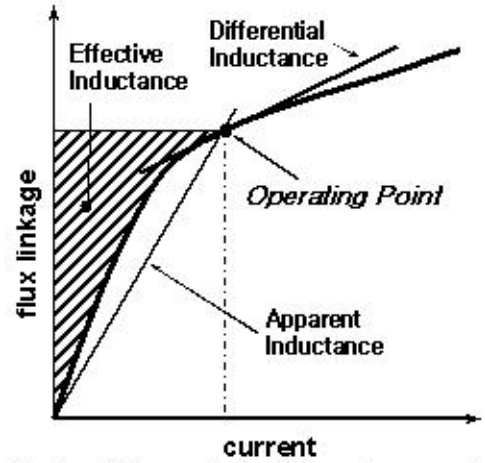


Fig. 7 Classification of inductance in flux linkage and current reference frame

not this problem. The filtered fundamental inductance in the VCM must be lower than the total inductance in the FPM. But for the both fundamental inductances, the difference between the inductances of the VCM and DFM accords with their definitions. The eliminated harmonic components in the FPM also can explain why the inductances calculated by 6 A current and 9 A current are almost the same.

As the above definitions, it is also known that both the calculated inductances in the FPM and VCM are the steady-state inductance, while those calculated by the DFM are the transient inductance. The steady-state inductance can be used to calculate the steady-state characteristics, such as the torque vs. speed waveform, efficiency map and so on. The transient inductance is produced when the current is varying. The dynamic analysis with PWM, program in the DSP of motor drive, and the other conditions with varying current are preferred to use the transient inductance.

#### IV. EXPERIMENT VERIFICATION

According to the previous calculation principles and electric circuit theory, some experiment methods for measuring the inductance of IPMSM and verifying the analysis results are derived.

##### A. Vector Control Method in Experiment

It is impossible to obtain the flux linkage in both no-load and load condition directly. However, the flux linkage can be calculated by Back-EMF with known speed. The flux linkage in the no-load condition is measured in zero d-axis current control, and calculated by (6)

$$\omega \psi_a = v_{q0} - R_q i_{q0} \quad (6)$$

where  $v_{q0}$  is the q-axis voltage generated by PI controller in steady state,  $i_{q0}$  is the measured q-axis current. And the d- and q-axis inductances are calculated by (7)

$$L_d = \frac{v_q - R_q i_q - \omega \psi_a}{\omega i_d}$$

$$L_d = \frac{(v_d - v_{d0}) - R_a i_d}{-\omega (i_q - i_{q0})} \quad (7)$$

where  $v_{d0}$  is the d-axis voltage in no-load condition. The  $v_{q0}, v_{d0}$  supply the energy losing in the mechanical losses under no-load condition. That is why they do not exist in theory equations.

### B. Differential Flux Linkage Method in Experiment

In VCM, the flux linkage under no-load condition is obtained by voltage and current. However, it is impossible to obtain the flux linkage under load condition in the same method, due to the Back-EMF. This problem has been solved by a locked-rotor method proposed in [3]. The brief procedure of this method for measuring  $L_q$  is:

1. lock the rotor at 0 position;
2. apply a stepwise voltage  $v_q$  and control  $i_d$  to constant;
3. measure the  $i_q$  and record the  $t$ ;
4. According to (8), the  $\Psi_q(t)$  can be calculated.

$$\Psi_q(t) = \int_0^t [v_q(\tau) - R_a i_q(\tau)] d\tau \quad (8)$$

5. According to (5), the q-axis inductance is calculated. The d-axis inductance can be measured and calculated in the same way.

### C. AC Standstill Method

Another experiment method named AC standstill method is mentioned in [8]. Unlike the previous two method, this method measures the phase self and mutual inductance, and hence the tested motor should have a neutral line. It also locks the rotor at a still position. And then apply an AC voltage with specific frequency between one phase terminal and the neutral terminal, meanwhile, measure the phase current and another phase voltage. After obtain the self- and mutual-inductance, the least square method and FFT are used to find the fundamental value and calculate the d- and q-axis inductances.

### D. Experiment Setting and Devices

In the differential flux linkage experiment method, the extra lock device and stepwise voltage controller make the experiment not ordinary. And it is evident that there is not current vector variation in the AC standstill method, i.e. this method can not present the cross-coupling effect. Due to these limitations, this paper adopts the vector control experiment method to verify the calculated inductance results. The experiment setting and devices are shown in Fig. 8. The motor is connected to a dynamometer, and operated at a specific speed. This speed is depending on the iron losses distribution. Because the analysis does not consider the current drop in the iron-loss resistance, the lower iron losses, the better results may be obtained. Before experiment, a reference d- and q-axis currents table for different current and current vector angle is calculated. Then, fix the q-axis current, and adjust the load torque until the d-axis current reaches the reference value. The experiment results measured in this way are shown as the star-lines in Fig. 6. It should be careful that it is not the corresponding experiment

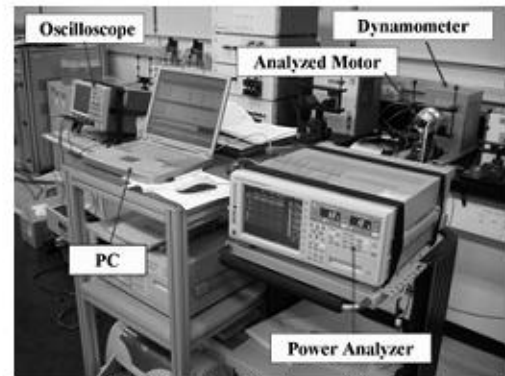


Fig. 8 Experiment setting and devices

results of the VCM. Because the PWM current regulation, it corresponds to the transient inductance, i.e. the results of DFM. Unfortunately, the experiment results and the calculated results are not well matched. The main reason is the experiment speed. The highest efficiency operating point of this spindle-type motor is at 26000 rpm. But the used motor drive in this paper only can drive the motor until 4000 rpm.

The inductances calculated by the VCM are not measured directly, because there is not absolute steady-state current. In this paper, an indirect method is adopted to verify the inductances. According to [9], a characteristic analysis is processed, the steady-state characteristics, such as torque vs. speed, d- and q-axis currents vs. speed, etc. can be obtained. In the experiment, specific a series of output torques and speeds, measure the magnitude of the corresponding d- and q-axis voltages and currents when the motor is in steady state. And then, compare the d- and q-axis voltages and currents respectively obtained from the characteristic analysis and experiment at the same torque vs. speed points. Fig. 9 (a) shows the comparison points, and (b)-(d) show the comparisons in voltage, current, efficiency, and losses. All comparison points in (b) and (c) are almost superposed. The calculated inductances by the VCM, i.e. the steady-state inductances are valid.

In Fig. 9 (d), it can be seen that the efficiency and losses have seriously differences between the analysis results and experiment results. This is the reason why the VCM experiment is failed to verify the inductances of the DFM. But in the characteristic analysis, the iron-losses resistance is taken account. Although it is not absolutely same to the real one, the influence can be reduced very much. That is why the comparisons in the characteristics are good working.

## V. CONCLUSION

This paper investigated the detail procedures of three major FEA inductance calculation methods for IPMSM, and analyzed the advantages and disadvantages of them. The computation time, complexity, and final results of these methods are compared and shown in Table II. According to the classification and definitions of inductance, the differences between the calculated inductances of any two methods are analyzed and explained. The inductances calculated by the FPM and VCM are regarded as the steady-state inductances, and they are preferred

to be used in the characteristic analysis. Those calculated by the DFM are the transient inductance, hence suitable for the dynamic analysis. Finally, the results of the VCM and DFM are verified by the corresponding experiment methods. Due to the influence of the iron-loss resistance, the direct measurement is difficult and inaccurate. The paper proposed and used an indirect verification method, and successfully verified the validity of the VCM.

REFERENCES

- [1] J. Y. Lee, S. H. Lee, G. H. Lee, and J. P. Hong, "Determination of parameters considering magnetic nonlinearity in an interior permanent magnet synchronous motor," *IEEE Trans. Magn.*, Vol. 42, No. 4, Apr. 2006.
- [2] G. H. Kang, J. P. Hong, G. T. Kim, and J. W. Park, "Improved parameter modeling of interior permanent magnet synchronous motor based on finite element analysis," *IEEE Trans. Magn.*, Vol. 36, No. 4, Jul. 2000.
- [3] B. Stumberger, G. Stumberger, D. Dolinar, etc., "Evaluation of saturation and cross-magnetization effects in interior permanent-magnet synchronous motor," *IEEE Trans. Ind. Appl.*, Vol. 39, No. 5, Sept./Oct. 2003.
- [4] E. C. Lovelace, T. M. Jahns, J. Wai, etc., "Design and experimental verification of a direct-drive interior PM synchronous machine using a saturable lumped-parameter model," *Ind. Appl. Conf.*, Vol. 4, pp. 2486-2492, Oct. 2002.
- [5] J. F. Gieras, E. Santini, and M. Wing, "Calculation of synchronous reactances of small permanent-magnet alternating-current motors: comparison of analytical approach and finite element method with measurements," *IEEE Trans. Magn.*, Vol. 34, No. 5, Sept. 1998.
- [6] T. A. Lipo, *Introduction to AC Machine Design (Vol. 1)*, WisPERC UW-Madison, 1996.
- [7] T. W. Nehl, F. A. Fouad, and N. A. Demerdash, "Determination of saturated values of rotating machinery incremental and apparent inductances by an energy perturbation method," *IEEE Trans. Power Appar. Syst.*, Vol. 101, Issue. 12, Dec. 1982.
- [8] R. Dutta, and M. F. Rahman, "A comparative analysis of two test methods of measuring d- and q-axis inductances of interior permanent magnet machine," *IEEE Trans. Magn.*, Vol. 42, No. 11, Nov. 2006.
- [9] Tao Sun, B. W. Kim, J. H. Lee, and J. P. Hong, "Determination of parameters of motor simulation module employed in ADVISOR," *IEEE Trans. Magn.*, Vol. 44, Issue. 6, June. 2008.

TABLE II  
COMPARISON OF COMPUTATION PROCESS

Method	Computation Time	Complexity
FPM	Fast	Simple
VCM	Slow	Complex
DFM	Very slow	Very complex

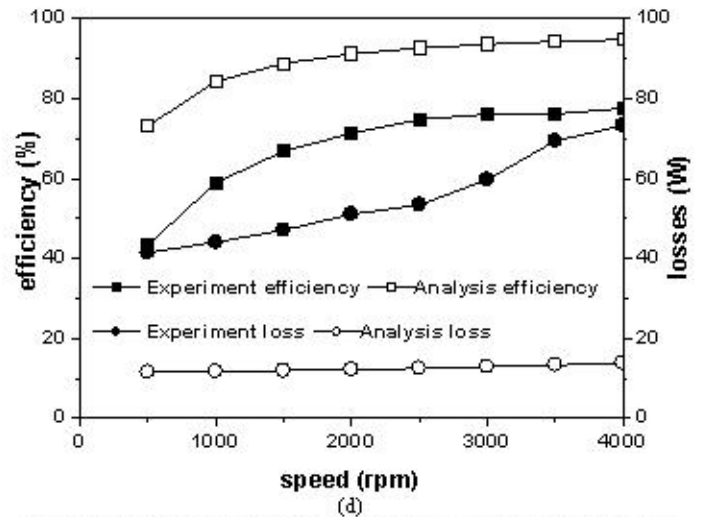
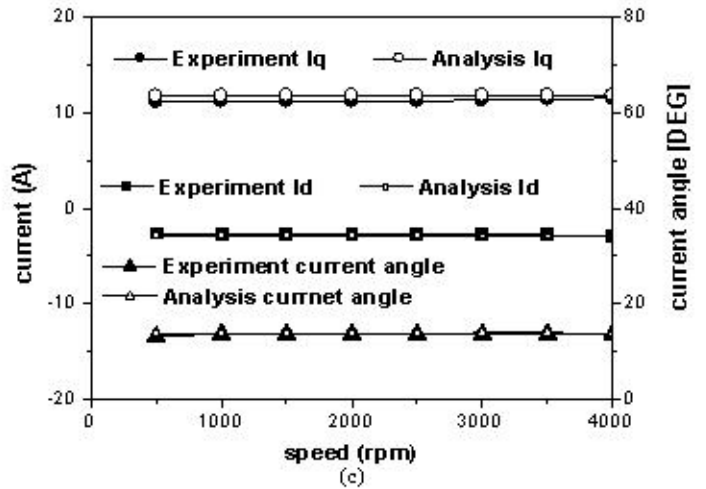
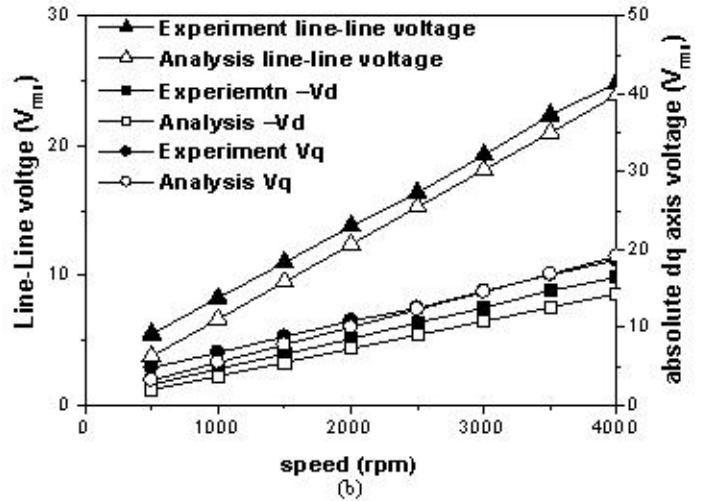


Fig. 9 Comparison of the analysis characteristics and experiment results: (a) comparison points in torque, power and speed, (b) comparison of line-line voltages and d- and q-axis voltages, (c) comparison of d- and q-axis currents, (d) comparison of efficiency and losses

